JACS Au
AN OPEN ACCESS JOURNAL OF THE AMERICAN CHEMICAL SOCIETY

pubs.acs.org/jacsau
Article

Enantioselective Desymmetrization of Trifluoromethylated Tertiary Benzhydrols via Hydrogen-Acceptor-Free Ir-Catalyzed Dehydrogenative C−H Silylation: Decisive Role of the Trifluoromethyl Group

Yoshihiko Yamamoto,* Ryu Tadano, and Takeshi Yasui

Cite This: *JACS Au* 2024, 4, 807−815
Read Online

ACCESS | Metrics & More | Article Recommendations | Supporting Information

ABSTRACT: Although the trifluoromethyl (CF_3) group is one of the most important fluorinated groups owing to its significant ability to modulate pharmacological properties, constructing trifluoromethylated stereogenic centers in an enantioselective manner has been a formidable challenge. Herein, we report the development of the enantioselective desymmetrization of trifluoromethylated benzhydrols via intramolecular dehydrogenative silylation using Ir catalysts with chiral pyridine-oxazoline (PyOX) ligands. The produced benzoxasilol was transformed into several unsymmetrical benzhydrols via iododesilylation and subsequent transition-metal-catalyzed cross-coupling reactions. Moreover, the same Ir catalyst system was used for the kinetic resolution of unsymmetrical trifluoromethylated benzhydrols.

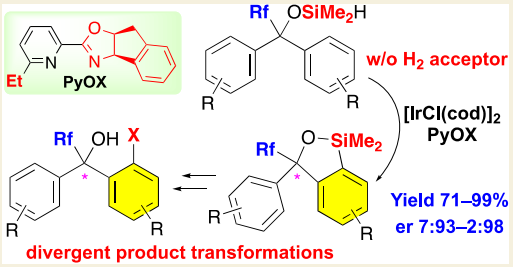

KEYWORDS: *asymmetric catalysis, C−H functionalization, fluorine, iridium catalyst, silane*

INTRODUCTION

The trifluoromethyl (CF_3) group is among the most important fluorinated groups owing to its ability to modulate pharmacological properties, such as membrane permeability, electrostatic/hydrophobic interactions with target receptors, and metabolic stability.[1] Accordingly, diverse methodologies have been developed to efficiently synthesize trifluoromethylated compounds; however, the synthesis of complex molecules, bearing CF_3 groups on tertiary or quaternary sp^3 carbons, has not been extensively investigated.[2] In particular, the enantioselective construction of trifluoromethylated stereogenic centers, which are found in bioactive compounds, such as reverse transcriptase inhibitors (efavirenz and its analogues)[3] and neurokinin-1 receptor antagonist CJ-17,493 (Figure 1a),[4] has been a formidable challenge.[5] Two strategies have been developed to enantioselectively construct trifluoromethylated tertiary alcohol motifs; the first involves the asymmetric additions of a nucleophile to a trifluoromethyl ketone, and the second involves the asymmetric trifluoromethylation of ketones (Figure 1a, inset scheme). In addition to these strategies that use conventional nucleophilic addition chemistry, the enantioselective desymmetrization of trifluoromethylated tertiary alcohols is a powerful method because optically active products can be obtained by catalytically differentiating enantiotopic groups remote from the trifluoromethylated Csp^3 center. Therefore, we investigated the enantioselective desymmetrization of trifluoromethylated benzhydrol **1** (Figure 1b). Our method has significant synthetic advantages; first, benzhydrol substrates can be prepared from readily available starting materials, and second, various optically active trifluoromethylated benzhydrols are accessible by transforming benzoxasilol products **3**. The latter is significant in terms of drug discovery because chiral 1,1-diarylmethane motifs are found in a diverse range of bioactive compounds.[6]

As a relevant example, Wang and co-workers recently reported the enantioselective desymmetrization of trifluoromethylated (isocyanomethylene)dibenzenes.[7] Although this method affords various 1,3-diaryl-1*H*-isoindole derivatives in high yields and enantioselectivities, an alternative method for accessing divergent optically active trifluoromethylated tertiary benzhydrols remains elusive. Although Hartwig and co-workers developed the Rh- or Ir-catalyzed enantioselective desymmetrization of benzhydrols via intramolecular dehydrogenative silylation, tertiary benzhydrols have not yet been investigated as substrates.[8] Moreover, the reaction of trifluoromethylated benzhydrols is challenging because the bulky and highly electron-withdrawing trifluoromethyl group strongly impacts the reactivity and selectivity of the enantioselective desymmetrization reaction. In fact, Zhang et al. demonstrated that the Ir-

Received: December 14, 2023
Revised: January 29, 2024
Accepted: January 30, 2024
Published: February 15, 2024

https://doi.org/10.1021/jacsau.3c00794
JACS Au 2024, 4, 807−815

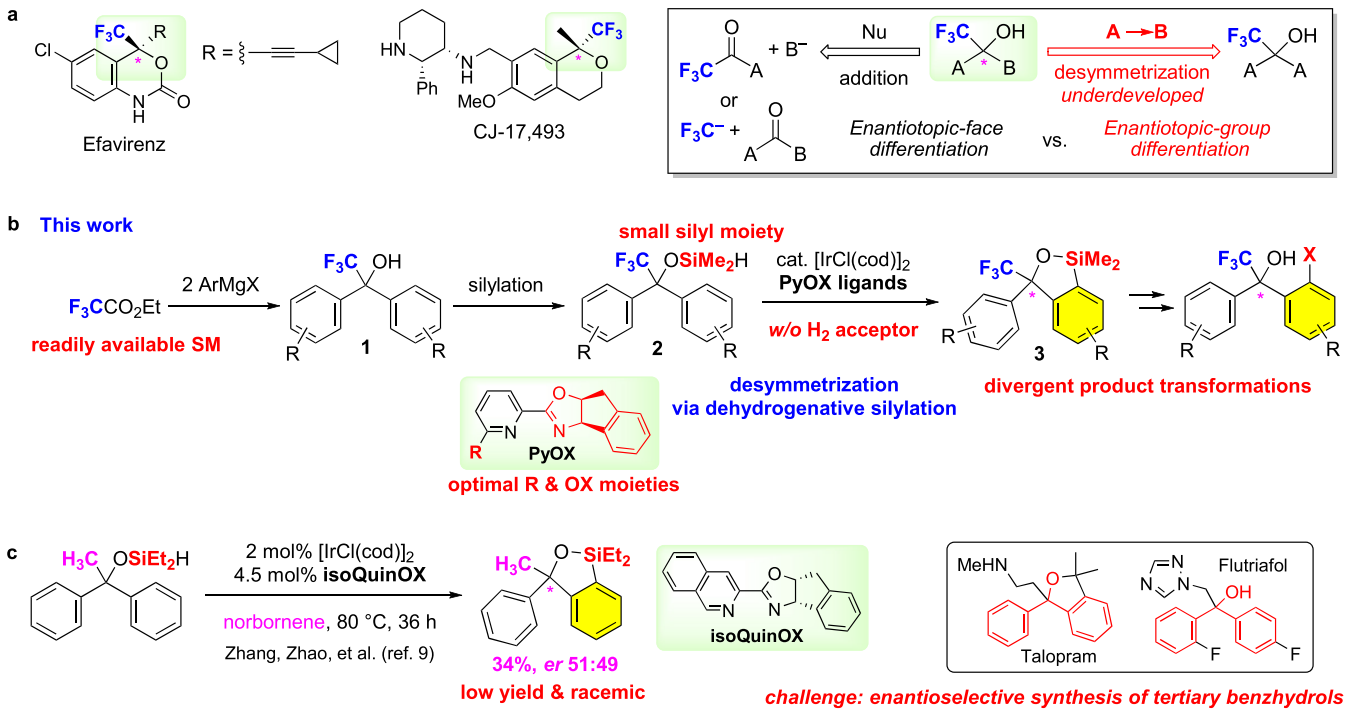

Figure 1. Background and our reaction design for catalytic desymmetrization of trifluoromethylated benzhydrols. (a) Bioactive compounds with trifluoromethylated tertiary stereogenic carbons and three methods for constructing trifluoromethylated tertiary alcohol motifs. (b) Our Ir-catalyzed enantioselective desymmetrization involving trifluoromethylated benzhydrols. (c) Previous Ir-catalyzed desymmetrization involving tertiary benzhydrol.

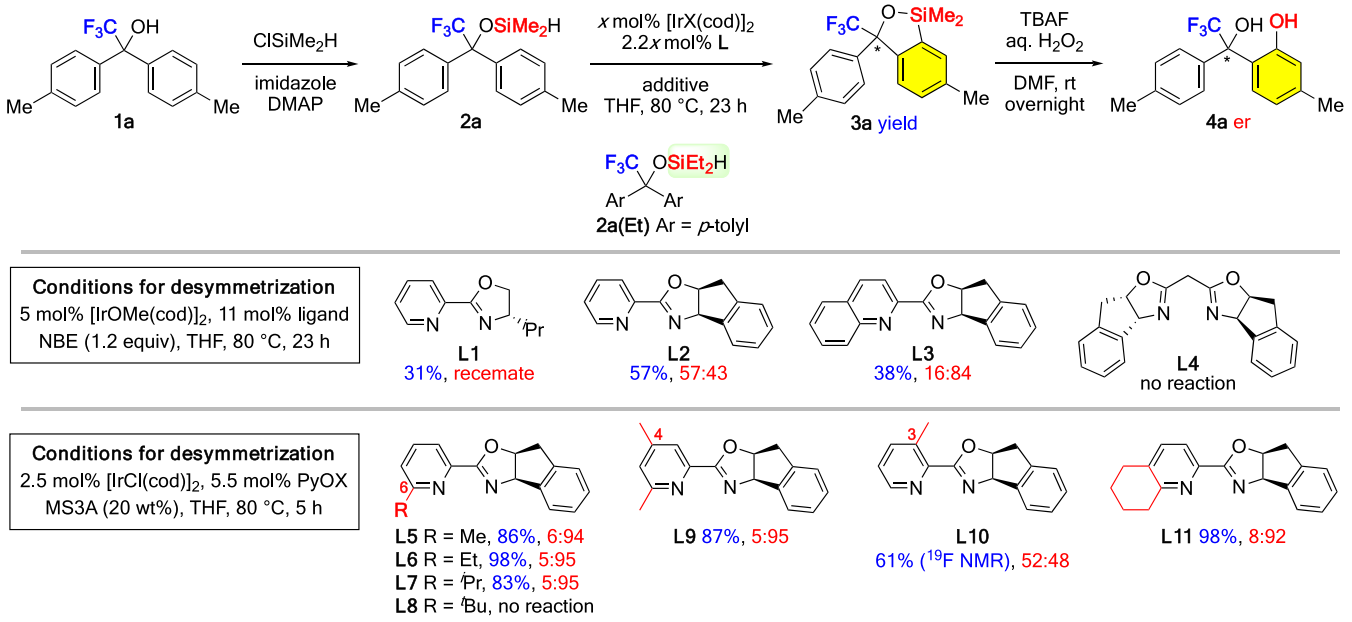

Figure 2. Ir-catalyzed intramolecular dehydrogenative silylation of **2a**.

catalyzed enantioselective desymmetrization of a tertiary benzhydrol derivative produced a racemic product in low yield (Figure 1c).[9] Therefore, we carefully optimized the reaction parameters, including the substrate silyl moiety, precatalysts, and chiral ligands, and found that Ir catalysts with chiral pyridine-oxazoline (PyOX) ligands are effective even in the absence of the hydrogen acceptor usually required for efficient dehydrogenative transformations (Figure 1b).

RESULTS AND DISCUSSION

Initial Optimization

Based on a report by Hartwig et al.,[8a] we initially investigated the Rh-catalyzed intramolecular dehydrogenative silylation of hydrosilane **2a**, which was obtained by the silylation of benzhydrol **1a** (Table S1, Supporting Information). The reaction of **2a** was performed in THF at 80 °C in the presence of 2.5 mol % $[RhCl(cod)]_2$, 5 mol % *rac*-BINAP, and norbornene (NBE, 1.2 equiv); however, these conditions

https://doi.org/10.1021/jacsau.3c00794
JACS Au 2024, 4, 807−815

afforded **3a** in only 24% yield (determined by ^{19}F NMR spectroscopy) and **2a** mostly remained unreacted (entry 1). The yield of **3a** significantly improved when less-polar hydrocarbon solvents (toluene and cyclohexane) were used (entries 4 and 5). Several chiral phosphine ligands were screened in cyclohexane (CyH; Figure S1, Supporting Information). Because **3a** is unsuitable for chiral high-performance liquid chromatography (HPLC) analysis, its enantioselectivity was determined after its conversion into more polar diol **4a** via Tamao oxidation. Almost no asymmetric induction was observed using bisphosphine ligands, such as BINAP, SEGPHOS, Phanephos, Chiraphos, Me-ferrocelane, and Josiphos. In addition, ^{t}Bu-Phox, MOP, and Monophos were ineffective ligands.

Therefore, Ir catalysis was investigated by performing the reaction of **2a** using 5 mol % $[IrOMe(cod)]_2$ and 11%11mol% chiral PyOX ligand because this type of chiral nitrogen ligand is readily available (Figure 2).[10] Although the use of PyOX-type ligand **L1** afforded **3a** as a racemate in low yield (31%), PyOX ligand **L2** bearing an indane-fused oxazoline moiety afforded a better yield (57%) albeit with a low enantiomeric ratio (57:43). Enantioselectivity improved (er 16:84) using quinoline-oxazoline ligand **L3**, although **3a** was produced in a lower yield (38%). In contrast, the symmetrical bis(oxazoline)-type ligand **L4** was ineffective.

Having obtained promising results, we next examined several reaction parameters for the Ir/PyOX-catalyzed intramolecular dehydrogenative silylation of **2a** (Figure 2 and Table 1). PyOX ligand **L2** was used in this optimization study, as its pyridine ring can be further modified to improve enantioselectivity. The desired product **3a** was obtained in 78% yield along with small amounts of **2a** and desilylation byproduct **1a** using a combination of $[IrOMe(cod)]_2$ and **L2** (Table 1, entry 1). A similar result was obtained using $[IrOMe(cod)]_2$/**L2** in the absence of NBE, showing that the hydrogen acceptor is unnecessary (entry 2). $[IrCl(cod)]_2$, the precursor of $[IrOMe(cod)]_2$, was used as a less expensive iridium source; however, a lower conversion of **2a** was observed (entry 3). Interestingly, a higher conversion of **2a** was obtained when NBE was omitted from the reaction by using $[IrCl(cod)]_2$ (entry 4). No trace of **1a** was observed in the absence of $[IrCl(cod)]_2$, which suggests that the Ir catalyst is involved in the desilylation of **2a** (entry 5). As adventitious water can promote desylilation, the reaction was conducted in the presence of a small amount of H_2O (5 μL), which led to a significantly lower conversion of **2a**, with an increased amount of **1a** observed (entry 6). This result implies that H_2O deactivates the catalyst. Therefore, MS3A was used to improve the catalytic efficiency by removing adventitious water from the reaction mixture (entry 7); gratifyingly, desilylation was effectively suppressed and the yield of **3a** increased to 94%, despite the lower catalyst loading (2.5 mol %). In contrast, **2a** was hardly consumed under similar conditions at 45 °C (entry 8). Therefore, an elevated reaction temperature (80 °C) is necessary for efficient reaction (see below). Moreover, the Ir-catalyzed dehydrogenative silylation of diethylsilane **2a(Et)** was found to be inefficient, as the corresponding product was formed in less than 15% yield, which indicates that the smaller dimethylsilyl group is optimal.

Table 1. Optimization of the Reaction Conditions for the Ir/L2-Catalyzed Reaction of 2a

entry	X	additive	**3a**/**2a**/**1a**[a]	**4a** er[b]
1	OMe	NBE (1.2 equiv)	78/4/4	57:43
2	OMe		79/4/4	58:42
3	Cl	NBE (1.2 equiv)	28/50/8	57:43
4	Cl		65/25/7	58:42
5			0/97/0	
6	Cl	H_2O (5 μL)	22/57/21	ND
7[c]	Cl	MS3A (20 wt %)	94/4/trace	58:42
8[c,d]	Cl	MS3A (20 wt %)	9/86/3	ND

[a]Determined by ^{19}F NMR analysis of crude mixture. [b]Determined after conversion of **3a** into **4a** using chiral HPLC (ND: not determined). [c]$[IrCl(cod)]_2$, 2.5 mol %; PyOX, 5.5 mol %; reaction time, 5 h. [d]Reaction was performed at 45 °C for 24 h.

The optimal ligand was identified by examining several PyOX-type ligands under the optimized conditions (Figure 2). PyOX ligands **L5**−**L7**, each bearing a substituent at position 6, exhibited similarly high efficiencies (83−98% yields, er 6:94−5:95). However, **L8**, with a bulky *tert*-butyl substituent, was ineffective. An additional methyl substituent at the 4-position in **L9** had almost no impact, whereas the use of 3-methyl analog **L10** resulted in almost no enantioselectivity. These results clearly demonstrate the importance of the substituents at position 6 of the pyridine ring. Finally, tetrahydroquinoline-based ligand **L11**, which was reported by Shi et al., was found to be an effective ligand under our conditions; however, slightly lower enantioselectivity (8:92) was observed. Accordingly, **L6**, bearing an ethyl substituent at the 6-position, was determined to be the optimal ligand because it afforded the best yield and enantioselectivity.

Substrate Scope

We next investigated the substrate scope of Ir-catalyzed asymmetric dehydrogenative silylation under the identified optimal conditions and subsequent Tamao oxidation in a telescoping manner (Figure 3). The dehydrogenative silylation of *p*-tolyl-substituted hydrosilane **2a** under standard conditions produced crude **3a** (96% ^{19}F NMR yield), which was directly subjected to Tamao oxidation to afford diol **4a** in 88% yield over two steps with a high enantiomeric ratio (5:95). Similarly, diols **4c**−**e**, bearing *tert*-butyl, phenyl, or methoxy substituents at the para-positions of the phenyl rings, were obtained in 88−96% yields with high enantiomeric ratios (4:96−3:97). Silane **2b** devoid of substituents on its phenyl rings, and silanes **2f**−**h**, bearing halogens at the para-positions, afforded the corresponding diols **4b** and **4f**−**h**, respectively, with high enantiomeric ratios, albeit in lower two-step yields (53−73%). Silanes **2i**−**k** with *meta*-substituted phenyl rings and 2-naphthyl derivative **2l** were also compatible with this telescoping method, with dehydrogenative silylation proceeding with high enantioselectivity (er 5:95−3:97); however, the Tamao oxidation of **3j**−**l** afforded the corresponding diols in moderate yields (40−52%). In contrast, *o*-tolyl derivative **2m** failed to afford **4m** under the same conditions, whereas the use of 5 mol % $[IrOMe(cod)]_2$ and 11 mol % **L6** in the presence of NBE under harsh conditions (2-MeTHF, 120 °C, sealed tube) produced **5m** in 67% yield through dehydrogenative silylation via benzylic C−H activation.[11] A CF_2H group was also compatible as **4n** was obtained in 91% yield with an enantiomeric ratio of 7:93. The introduction of a bulkier C_2F_5 group led to lower yields of both intermediate **3o** (71%) and final product **4o** (56%), although a higher enantiomeric ratio (2:98) was obtained compared to that of **4b** (5:95). Moreover,

https://doi.org/10.1021/jacsau.3c00794
JACS Au 2024, 4, 807−815

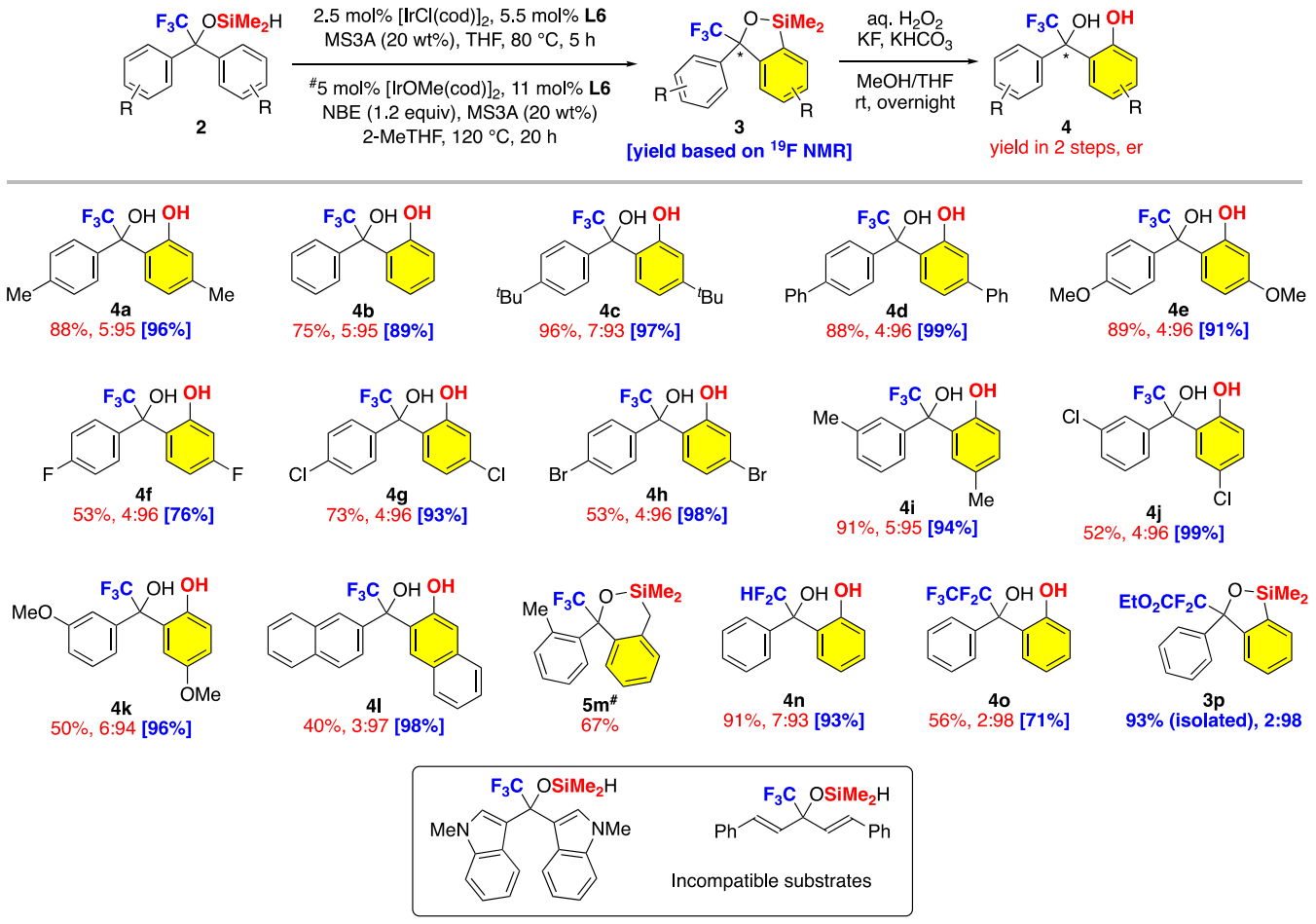

Figure 3. Substrate scope of Ir-catalyzed asymmetric dehydrogenative silylation, followed by Tamao oxidation. Yields of isolated products over two steps are indicated along with enantiomeric ratios (er) determined by chiral HPLC analysis (red, nd: not determined). Crude yields of benzoxasilols **3** determined by ^{19}F NMR spectroscopy are indicated in parentheses (blue).

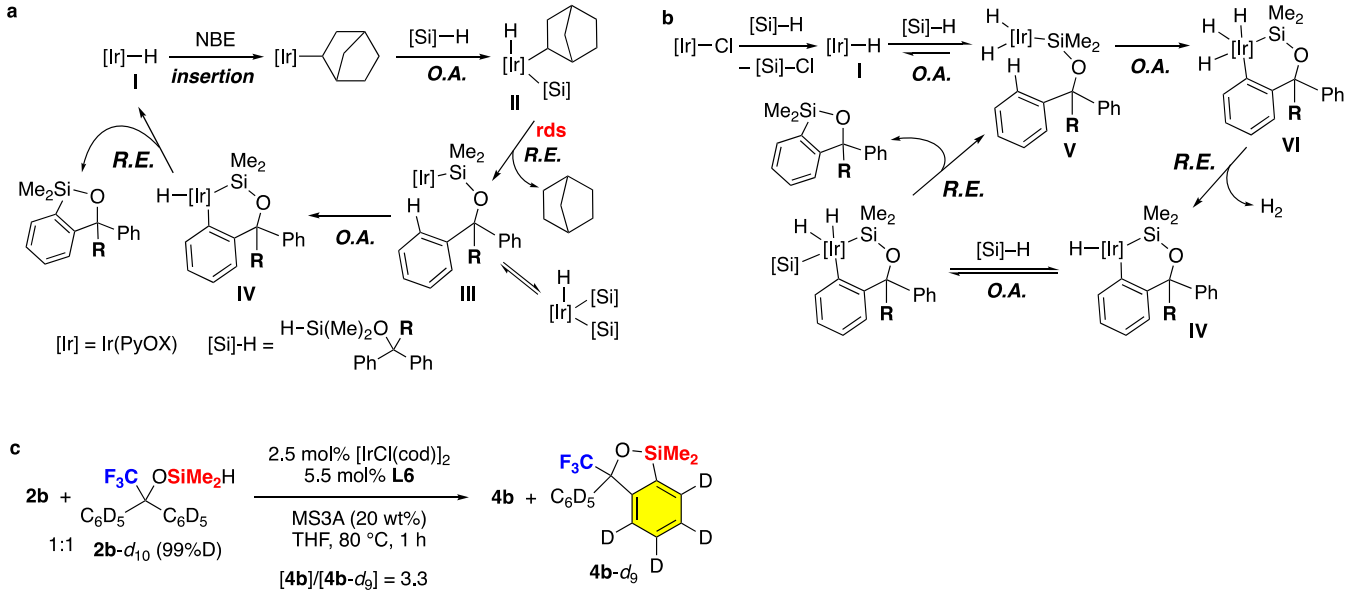

Figure 4. Mechanistic proposal. (a) Plausible catalytic cycle in the presence of NBE. (b) Alternative catalytic cycle in the absence of NBE. (c) Reaction with deuterated substrate **2b**-d_{10}.

substrate **2p** bearing a CF_2CO_2Et group afforded benzoxasilol **3p** in 93% yield, which was directly used to determine the enantiomeric ratio (2:98). Bis(3-indolyl) and dialkenyl methanol derivatives were also subjected to dehydrosilylation; however, the former exhibited no reactivity, and the latter led to partial decomposition.

https://doi.org/10.1021/jacsau.3c00794
JACS Au 2024, 4, 807–815

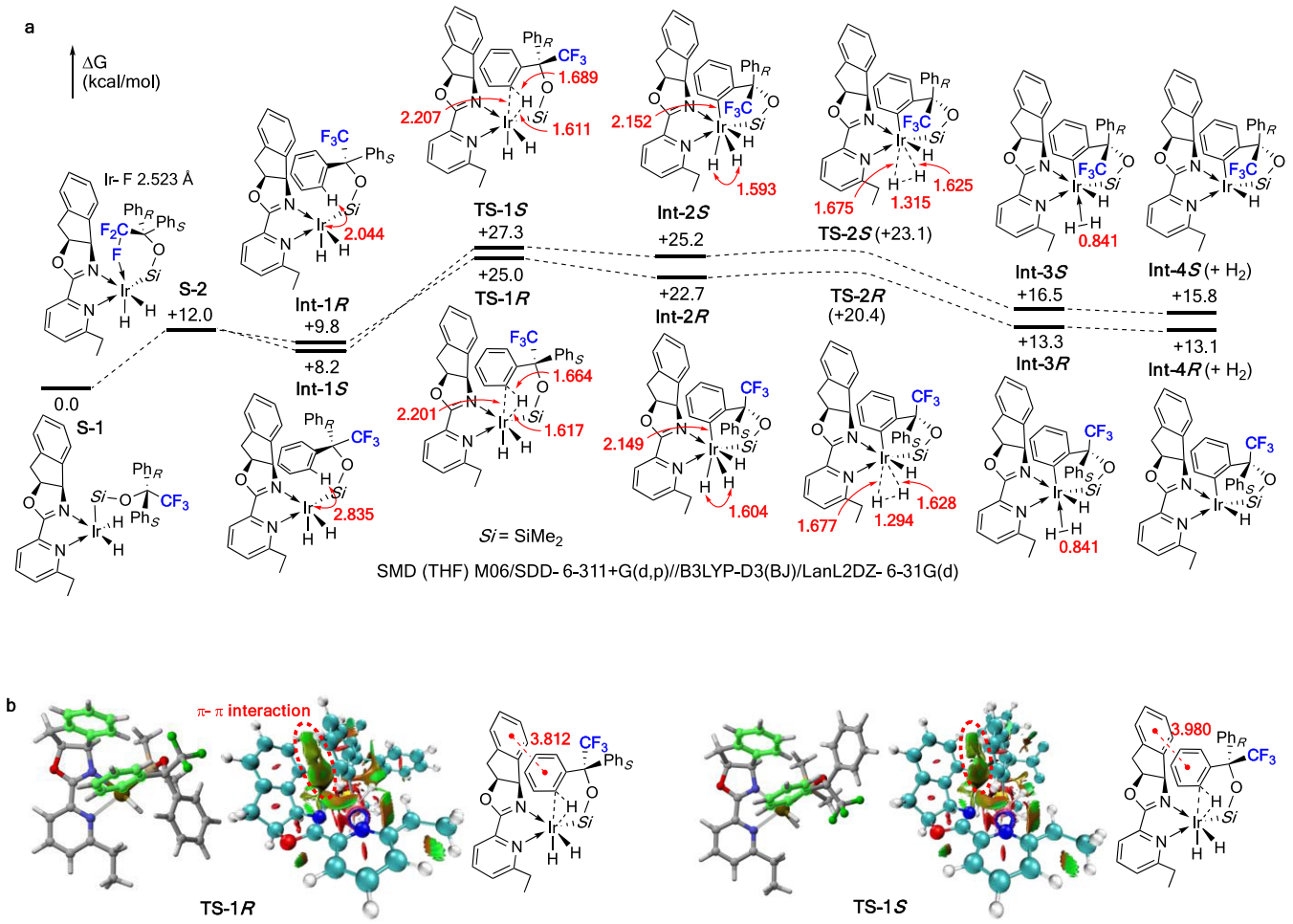

Figure 5. Computational studies. (a) DFT analysis of the C−H activation step. (b) NCI analyses of **TS-1*R*** and **TS-1*S***.

Mechanistic Investigations

Based on the kinetic isotope effects (KIEs) observed in related Ir-catalyzed desymmetrization involving benzhydrol derivatives, Hartwig and Shi proposed a plausible catalytic cycle in the presence of NBE (R = H, Figure 4a).[8b] The oxidative addition (O.A.) of the silane substrate is reversible because no KIE was observed. The catalytic cycle starts with the insertion of NBE into iridium hydride species **I** followed by the O.A. of a hydrosilane substrate to generate alkyl hydride species **II**. Subsequent reductive elimination (R.E.) of norbornane from **II** is considered to be the rate-determining step.[8b] The resultant coordinatively unsaturated silyliridium(I) species **III** undergoes O.A. with the *ortho* C−H bond of a phenyl substituent to produce Ir(III) metallacyclic intermediate **IV**. The final R.E. event regenerates Ir(I) hydride **I** with the concomitant formation of a benzoxasilol product. In contrast to the previous methods,[8] no hydrogen acceptor is required for the dehydrogenative silylation of the trifluoromethylated benzhydrol derivatives in this study. Therefore, an alternative catalytic cycle that operates in the absence of NBE needs to be considered (Figure 4b). The reaction of a chloroiridium(I) precatalyst with the hydrosilane substrate produces iridium(I) hydride **I**,[12] which undergo facile O.A. of the hydrosilane substrate to generate Ir(III) dihydride species **V**.[13,14] The subsequent *ortho* C−H O.A. of Ir(III) dihydride species **V**, which is the rate- and enantioselectivity-determining step, produces Ir(V) metallacyclic intermediate **VI**. A 1:1 mixture of **2b** and **2b**-d_{10} was allowed to react under the standard conditions for 1 h (Figure 4c). The ^{19}F NMR spectrum of the crude reaction mixture revealed that benzoxasilol products **4b** and **4b**-d_9 were formed in a 3.3:1 ratio, which suggests that the C−H activation step has an unignored effect on the overall reaction rate. Facile reductive elimination of H_2 generates Ir(III) metallacyclic intermediate **IV** that then undergoes O.A. with another silane substrate and subsequent R.E. of the benzoxasilol product.[15]

While elucidating the details of the reaction mechanism requires further research, we used computational techniques to gain insight into the C−H activation step (Figure 5a). Density functional theory (DFT) calculations at the SMD (THF) M06/SDD−6-311+G(d,p)//B3LYP-D3(BJ)/LanL2DZ−6-31G(d) level of theory (for details, see the Supporting Information) afforded Ir(III) dihydride complex **S-1**, which has a square pyramidal geometry with a silyl ligand at the apical position, as the starting point. Geometrical isomerization of **S-1** leads to the less-stable dihydride complex **S-2** in which the silyl ligand is *cis* to the ligand oxazolyl moiety; **S-2** further evolves into the slightly more stable intermediates **Int-1*R*** and **Int-1*S*** via C−O bond rotation. The transition states for O.A. of the *ortho* C−H bonds were located as **TS-1*R*** and **TS-1*S***, with activation barriers of 15.2 and 19.1 kcal/mol from **Int-1*R*** and **Int-1*S***, respectively. The formations of Ir(V) trihydride intermediates **Int-2*R*** and **Int-2*S*** are endergonic (12.9 and 17.0 kcal/mol, respectively). While the transition states for the

https://doi.org/10.1021/jacsau.3c00794
JACS Au 2024, 4, 807−815

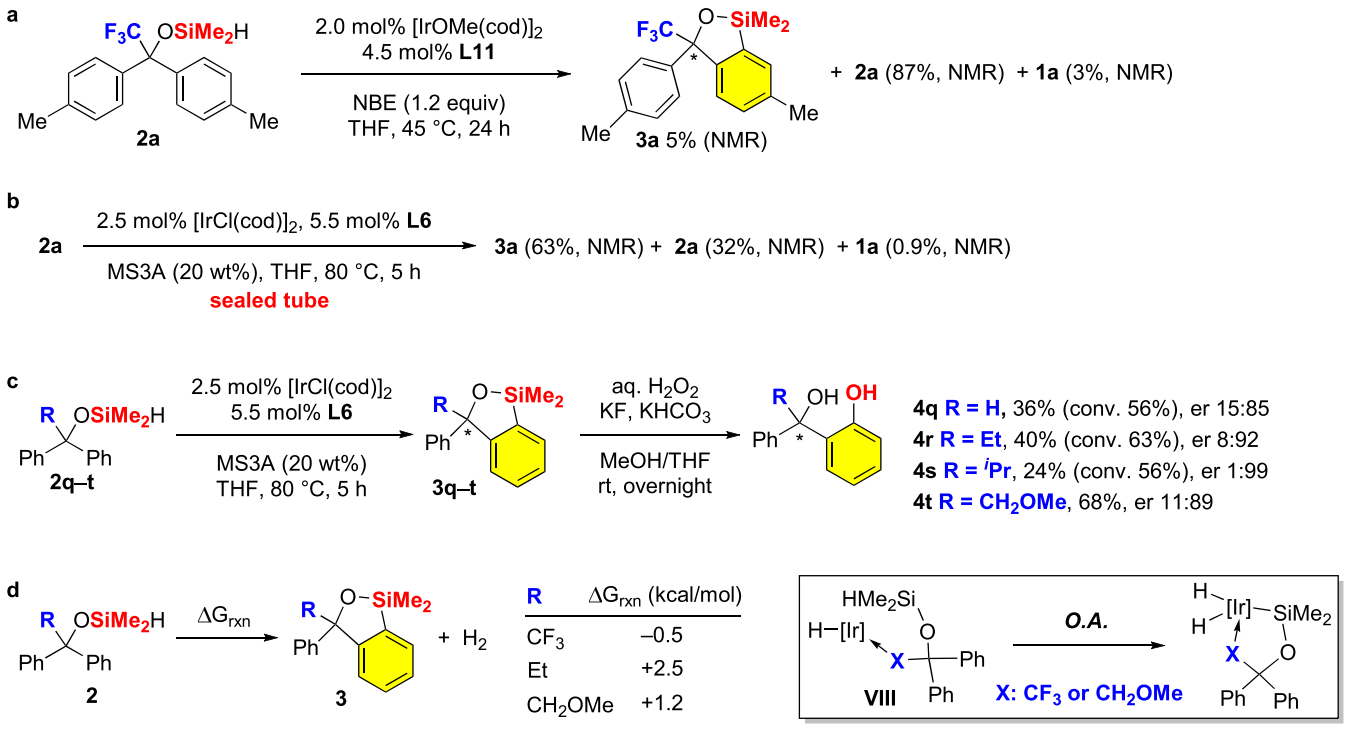

Figure 6. Control experiments. (a) Reaction of **2a** under Hartwig and Shi's conditions. (b) Reaction of **2a** under our conditions using a sealed tube. (c) Reactions of nonfluorinated benzhydrol derivatives. (d) Change in Gibbs energies for the transformations of **2** into **3** and H_2.

subsequent H_2 reductive elimination (**TS-2*R*** and **TS-2*S***) were located, their Gibbs energies were lower than those of **Int-2*R*** and **Int-2*S***, respectively; consequently, reductive elimination of H_2 from **Int-2*R*** and **Int-2*S*** is barrierless, which leads to the exergonic (9.4 and 8.7 kcal/mol) formation of Ir(III) σ-H_2 complexes **Int-3*R*** and **Int-3*S***, respectively. Although the C−H activation steps leading to Ir(III) σ-H_2 complexes are endergonic and reversible, facile extrusion of H_2 gas from the reaction solutions at elevated temperatures renders the overall reaction irreversible.

The energetic span between **S-1** and **TS-1*R*** (25.0 kcal/mol) is lower than that between **S-1** and **TS-1*S*** (27.3 kcal/mol); hence, the (*R*) enantiomer is predicted to be favored. This result was corroborated by the X-ray diffraction (XRD) study of a product (see below). The enantiomeric ratio was theoretically determined to be (*R*):(*S*) = 96:4 at 80 °C from the difference in the activation barriers associated with **TS-1*R*** and **TS-1*S*** ($\Delta\Delta G^{\ddagger}$ = 2.3 kcal/mol), which is in good agreement with the experimentally observed enantiomeric ratio of 95:5. **TS-1*R*** and **TS-1*S*** were subjected to noncovalent interaction (NCI) analysis.[16] The green regions reveal π−π interactions between the benzene rings in the ligand and substrate (highlighted) in these TSs (Figure 5b). The π−π interactions are expected to be more efficient in **TS-1*R*** than in **TS-1*S*** because the distance between the two benzene rings is shorter in the former. Accordingly, **TS-1*R*** is favored over **TS-1*S***, leading to the (*R*)-enantiomer being the major product. These analyses reveal that the ligand indenyl moiety plays an important role in stabilizing each TS. In fact, the C−H activation that proceeds from the face opposite to the ligand indenyl moiety is disfavored because the energetic span between **S-1** and **TS-3*R*** or **TS-3*S*** is +31.7 and +28.7 kcal/mol, respectively (Figure S2, Supporting Information).

The influence of the C6 substituent of the PyOX ligands on the enantioselectivity is noteworthy (Figure 2). We located the C−H activation TSs involving **L2** without the C6 substituent [**TS-1*R*-(H)** and **TS-1*S*-(H)**] and **L5** with the methyl group at the 6-position [**TS-1*R*-(Me)** and **TS-1*S*-(Me)**], and their geometries were compared with those of **TS-1*R*** and **TS-1*S*** (Figure S3, Supporting Information). As a general trend, the Ir−N(Py) distances (l_1) are longer than those of Ir−N(Ox) (l_2) in these TSs. The difference between l_1 and l_2 decreased in the order **TS-1*R*/TS-1*S*** > **TS-1*R*-(Me)/TS-1*S*-(Me)** ≫ **TS-1*R*-(H)/TS-1*S*-(H)** because of the steric repulsion of the C6 alkyl groups of **L6** and **L5**. Moreover, the same trend was found in the distance between the benzene rings in the PyOX ligand and substrate. These results qualitatively correlate with the experimentally observed order of enantioselectivity. However, the theoretical enantiomeric ratio (94:6) based on the energy difference between **TS-1*R*-(H)** and **TS-1*S*-(H)** ($\Delta\Delta G^{\ddagger}$ = +1.96 kcal/mol) is much larger than that observed experimentally (58:42). Therefore, further investigation is needed to elucidate the role of the C6 substituents.

Although the above C−H activation step from the Ir(III) dihydride intermediate (**Int-1*R***) is facile, an alternative C−H activation step involving an Ir(I) species generated via H_2 reductive elimination from **Int-1*R*** is conceivable. However, the activation barrier of the H_2 reductive elimination from **Int-1*R*** ($\Delta G^{\ddagger}$ = +36.0 kcal/mol) is too high to overcome under the experimental conditions (Figure S4a, Supporting Information). The final R.E. of the benzoxasilol product from Ir(III) metallacyclic intermediate (**Int-4*R***) proceeds with a resonable activation barrier of $\Delta G^{\ddagger}$ = +23.9 kcal/mol (Figure S4b, Supporting Information); however, the R.E. step involving Ir(V) metallacyclic intermediate (**Int-10*R***), which is generated via the O.A. of the hydrosilane substrate to **Int-4*R***, was found to be barrierless (Figure S4c, Supporting Information). These results support the proposed Ir(III)/Ir(V) catalytic cycle as outlined in Figure 4b.[17]

https://doi.org/10.1021/jacsau.3c00794
JACS Au 2024, 4, 807−815

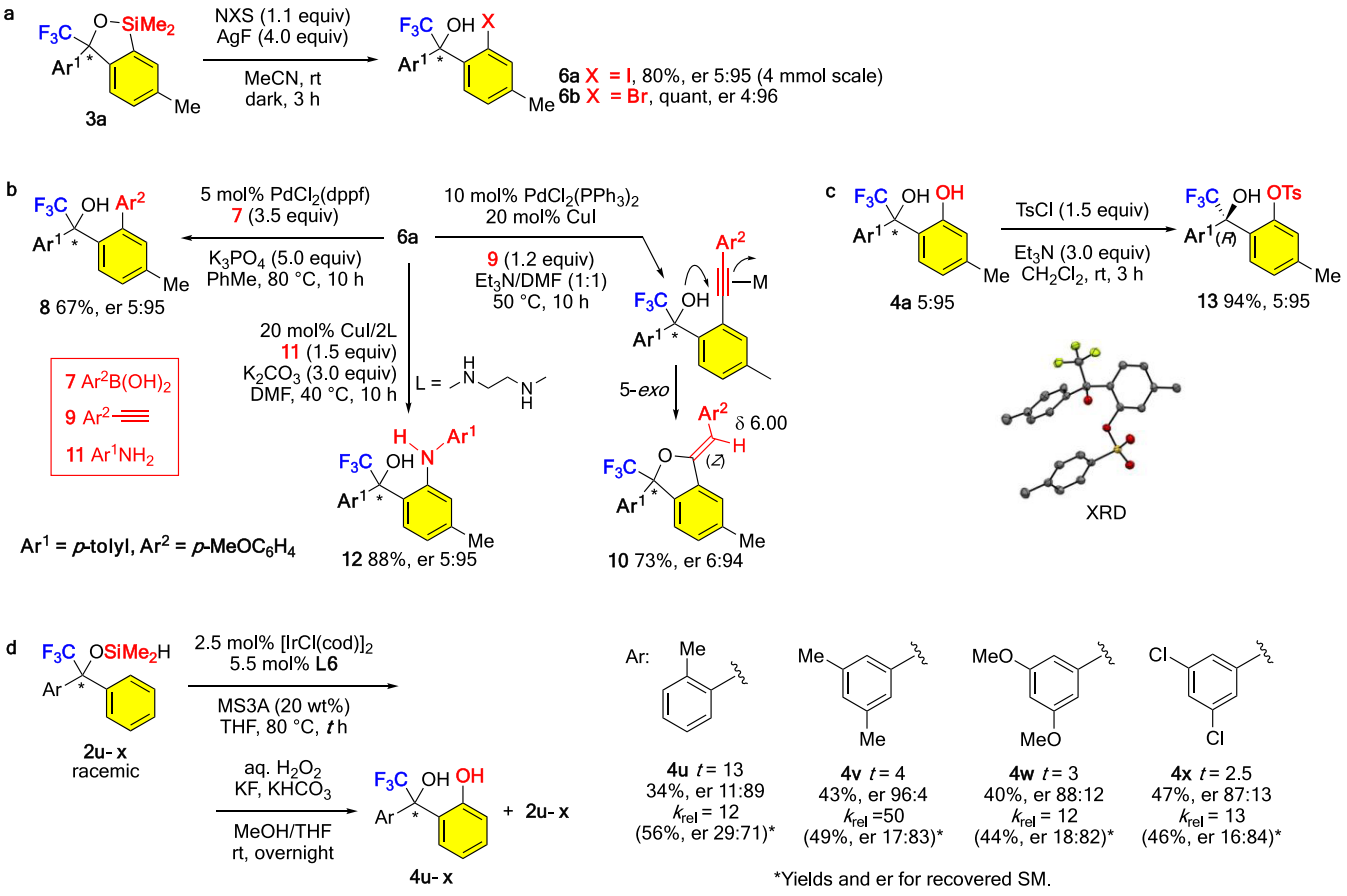

Figure 7. Synthetic applications. (a) Halodesilylation of **3a**. (b) Transition-metal-catalyzed transformations of iodide **6a** into chiral trifluoromethylated benzhydrol derivatives. (c) Preparation of tosylate **13** and its crystal structure. (d) Kinetic resolution of unsymmetrical benzhydrol derivatives. Relative rate k_{rel} was determined using the equation: $k_{rel} = \ln[1 - c(1 + ee_p)]/\ln[1 - c(1-ee_p)]$ (c: conversion based on product yields, ee_p: product enantiomeric excess).

To shed light on the role of the CF_3 group, several control experiments were conducted (Figure 6). The reaction of trifluoromethylated benzhydrol derivatives **2a** hardly proceeded under the conditions reported by Shi et al. (Figure 6a). Because ligand **L11** was efficient under our conditions, an elevated reaction temperature is required for benzhydrol substrates bearing the bulky CF_3 group. We assumed that the elevated reaction temperature facilitated the C−H activation step by extrusion of H_2 from the reaction solution to the gas phase. In fact, the reaction of **2a** performed in a sealed tube under our conditions resulted in diminished substrate conversion (Figure 6b). Then, nonfluorinated benzhydrols were subjected to Ir-catalyzed asymmetric dehydrogenative silylation and subsequent Tamao oxidation (Figure 6c). Secondary benzhydrol derivative **2q** (R = H) exhibited low conversion (56%), with an enantiomeric ratio of 15:85 observed after Tamao oxidation, which is lower than that of the corresponding CF_3-substituted analogue **4b** (5:95). The CF_3 group is comparable in size to the ethyl and isopropyl groups rather than the methyl group.[18] Indeed, the van der Waals volume of the CF_3 group (39.8 Å^3) is closer to that of an ethyl group (38.9 Å^3) than that of a methyl group (21.6 Å^3), and the *A* value of the CF_3 group (2.10 kcal/mol) is similar to that of an isopropyl group (2.15 kcal/mol), while those of the methyl and ethyl groups are smaller (1.70 kcal/mol). Consistent with these data, higher enantiomeric ratios were obtained in the reactions of tertiary benzhydrol derivatives **2r** (R = Et, er 8:92) and **2s** (R = ^{i}Pr, er 1:99) than that of **2q**, although the conversions of less than 63% were observed. In striking contrast, methoxymethyl-containing benzhydrol derivative **2t** was converted into **4t** in 68% yield over two steps, with a moderate enantiomeric ratio of 11:89 observed. These results highlight the importance of a heteroatom γ to the siloxy group in this Ir-catalyzed dehydrogenative silylation. We evaluated changes in Gibbs energies for the transformations of silanes **2** into benzoxasilols **3** and H_2 (Figure 6d). The transformation of **2b** (R = CF_3) into **3b** and H_2 was calculated to be slightly exergonic (−0.5 kcal/mol), while that of **2r** (R = Et) into **3r** and H_2 is endergonic by 2.5 kcal/mol, and the transformation of **2t** (R = CH_2OMe) into **3t** and H_2 was determined to be less endergonic (1.2 kcal/mol). These thermodynamic data are in good qualitative agreement with the observed reaction efficiencies: **2b** > **2t** ≫ **2r**. We also hypothesize that the coordinating groups assist silane O.A. by placing the Si−H bond in close proximity to the Ir center (Figure 6d, inset scheme).

Synthetic Applications

To demonstrate the synthetic potential of our method, we divergently transformed **3a** into a representative product. According to a previous report,[8a] **3a** was treated with NIS or NBS in the presence of AgF (excess) in acetonitrile at room temperature to afford the desired iodide **6a** or bromide **6b** in high yields without significant erosion of the enantiomeric ratio (Figure 7a), after which **6a** was subjected to transition-metal-

https://doi.org/10.1021/jacsau.3c00794
JACS Au 2024, 4, 807−815

catalyzed cross-coupling reactions (Figure 7b). The Suzuki−Miyaura coupling of **6a** with *p*-anisylboronic acid (**7**) afforded the biaryl product **8** in 67% yield. The Sonogashira−Hagihara coupling of **6a** with 1-ethynyl-4-methoxybenzene (**9**) produced (*Z*)-benzylidenephthalan derivative **10** in 73% yield via 5-*exo* cyclization of the initially formed diarylalkyne intermediate.[19] In addition to these C−C coupling reactions, Ullmann coupling of **6a** with *p*-toluidine (**11**) afforded diarylamine derivative **12** in 88% yield. Importantly, enantiomeric purity was maintained in all coupling reactions. The phenol moiety of **4a** was tosylated using *p*-tosyl chloride and Et_3N to afford **13** in 94% yield with an intact enantiomeric ratio (Figure 7c). Because good-quality single crystals of **13** were obtained, their absolute configuration was determined to be (*R*) by XRD.[20]

Finally, we briefly investigated the kinetic resolution of unsymmetrical substrates **2u−x** using the Ir/PyOX catalyst system (Figure 7d). Because *o*-tolyl derivative **2m** did not undergo dehydrogenative silylation under the standard conditions, benzhydrol derivative **2u** bearing *o*-tolyl and phenyl substituents was subjected to Ir-catalyzed dehydrogenative silylation for 13 h. After Tamao oxidation, phenol derivative **4u** was obtained in 34% yield with a moderate enantiomeric ratio of 11:89. In contrast, a benzhydrol derivative bearing an *o*-methoxyphenyl substituent failed to undergo dehydrogenative silylation. Therefore, we examined benzhydrol derivatives bearing 3,5-disubstituted phenyl substituents as substrates. Dehydrogenative silylation of **2v** bearing 3,5-xylyl substituent was conducted for 4 h, and the subsequent Tamao oxidation afforded phenol derivative **4v** in 43% yield with a higher enantiomeric ratio of 96:4. 3,5-Dimethoxyphenyl derivative **2w** and 3,5-dichlorophenyl derivative **2x** were also compatible with the kinetic resolution conditions; the corresponding products **4w** and **4x** were produced in 40% and 47% yields, respectively, and with moderate enantiomeric purities (er = 88:12 and 87:13, respectively).

CONCLUSIONS

We successfully realized the enantioselective desymmetrization of trifluoromethylated benzhydrols via intramolecular dehydrogenative silylation using Ir catalysts and chiral PyOX ligands. No hydrogen acceptor was required for the present enantioselective desymmetrization of trifluoromethylated benzhydrols, unlike previous Rh- or Ir-catalyzed methods, which require norbornene as the hydrogen acceptor. The mechanism responsible for differentiating the enantiotopic aryl *ortho* C−H bonds was examined using DFT calculations. The produced benzoxasilol can be transformed into several unsymmetrical benzhydrols via iododesilylation, followed by transition-metal-catalyzed cross-coupling reactions. Moreover, the same Ir/PyOX catalyst system was applied to the kinetic resolution of unsymmetrical trifluoromethylated benzhydrols.

METHODS

Representative Procedure for Sequential Intramolecular Dehydrogenative Silylation/Tamao−Fleming Oxidation

A solution of silyl ether **2a** (67.6 mg, 0.200 mmol), $[IrCl(cod)]_2$ (3.4 mg, 0.00506 mmol), PyOX ligand **L6** (2.9 mg, 0.0110 mmol), and MS3A (0.2 g) in dry THF (1 mL) was degassed at −90 °C and then stirred at 80 °C for 5 h under an Ar atmosphere. The volatile materials were evaporated in vacuo, and the obtained crude product was filtered through a short-pass silica gel column (hexane/AcOEt, 10/1). The crude yield of **3a** (96%) was evaluated by ^{19}F NMR using trifluorotoluene as an internal standard.

To crude **3a** were added $KHCO_3$ (62.8 mg, 0.627 mmol), KF (37.0 mg, 0.637 mmol), MeOH (0.5 mL), THF (0.5 mL), and aq. H_2O_2 (ca. 34.5%, 0.2 mL, ca. 2 mmol), and the mixture was stirred at room temperature for 12 h. The reaction was quenched by adding portionwise $Na_2S_2O_3{\cdot}5H_2O$ (0.3 g). The mixture was stirred at room temperature for 30 min. The mixture was filtered through a pad of Celite, and insoluble materials were washed with ether (10 mL). The solvents were evaporated in vacuo, and the obtained crude product was purified by silica gel column chromatography (hexane/AcOEt, 98:2−94:6) to afford **4a** (52.2 mg, 88%, er 5:95) as a colorless oil.

ASSOCIATED CONTENT

Supporting Information

The Supporting Information is available free of charge at https://pubs.acs.org/doi/10.1021/jacsau.3c00794.

Experimental details; characterization data for all new compounds; DFT calculation data; and HPLC and NMR charts (PDF)

X-ray crystallographic data for **13** (CIF)

AUTHOR INFORMATION

Corresponding Author

Yoshihiko Yamamoto − *Department of Basic Medicinal Sciences, Graduate School of Pharmaceutical Sciences, Nagoya University, Chikusa, Nagoya 464-8601, Japan;* orcid.org/0000-0001-8544-6324; Email: yamamoto-yoshi@ps.nagoya-u.ac.jp

Authors

Ryu Tadano − *Department of Basic Medicinal Sciences, Graduate School of Pharmaceutical Sciences, Nagoya University, Chikusa, Nagoya 464-8601, Japan*

Takeshi Yasui − *Department of Basic Medicinal Sciences, Graduate School of Pharmaceutical Sciences, Nagoya University, Chikusa, Nagoya 464-8601, Japan;* orcid.org/0000-0002-7630-8736

Complete contact information is available at: https://pubs.acs.org/10.1021/jacsau.3c00794

Author Contributions

CRediT: **Yoshihiko Yamamoto** conceptualization, data curation, project administration, writing-original draft; **Ryu Tadano** data curation, investigation, writing-review & editing; **Takeshi Yasui** validation, writing-review & editing.

Notes

The authors declare no competing financial interest.

ACKNOWLEDGMENTS

This research was partially supported by the Platform Project for Supporting Drug Discovery and Life Science Research (Basis for Supporting Innovative Drug Discovery and Life Science Research (BINDS) from AMED under Grant Number JP23ama121044) and JSPS KAKENHI (Grant Number JP 22K05110). Computations were performed using the Research Center for Computational Science, Okazaki, Japan (Project: 22-IMS-C242, 23-IMS-C125). R.T. acknowledges the Interdisciplinary Frontier Next-Generation Researcher Program of the Tokai Higher Education and Research System.

REFERENCES

(1) (a) Müller, K.; Faeh, C.; Diederich, F. Fluorine in Pharmaceuticals: Looking Beyond Intuition. *Science* **2007**, *317*, 1881−1886. (b) Purser, S.; Moore, P. R.; Swallow, S.; Gouverneur, V. Fluorine in medicinal chemistry. *Chem. Soc. Rev.* **2008**, *37*, 320−330.

(2) Selected reviews: (a) Ma, J.-A.; Cahard, D. Strategies for nucleophilic, and radical trifluoromethylations. *J. Fluorine Chem.* **2007**, *128*, 975−996. (b) Liu, H.; Gu, Z.; Jiang, X. Direct Trifluoromethylation of the C−H Bond. *Adv. Synth. Catal.* **2013**, *355*, 617−626. (c) Zhu, W.; Wang, J.; Wang, S.; Gu, Z.; Aceña, J. L.; Izawa, K.; Liu, H.; Soloshonok, V. A. Recent advances in the trifluoromethylation methodology and new CF_3-containing drugs. *J. Fluorine Chem.* **2014**, *167*, 37−54. (d) Barata-Vallejo, S.; Postigo, A. New Visible-Light-Triggered Photocatalytic Trifluoromethylation Reactions of Carbon−Carbon Multiple Bonds and (Hetero)Aromatic Compounds. *Chem. - Eur. J.* **2020**, *26*, 1065−11084. (e) Aradi, K.; Kiss, L. Carbotrifluoromethylations of C−C Multiple Bonds (Excluding Aryl- and Alkynyltrifluoromethylations). *Chem. - Eur. J.* **2023**, *29*, No. e202203499. (f) Kawamura, S.; Barrio, P.; Fustero, S.; Escorihuela, J.; Han, J.; Soloshonok, V. A.; Sodeoka, M. Evolution and Future of Hetero- and Hydro-Trifluoromethylations of Unsaturated C−C bonds. *Adv. Synth. Catal.* **2023**, *365*, 398−462.

(3) (a) Li, S.; Ma, J.-A. Core-structure-inspired asymmetric addition reactions: enantioselective synthesis of dihydrobenzoxazinone- and dihydroquinazolinonne-based anti-HIV agents. *Chem. Soc. Rev.* **2015**, *44*, 7439−7448. (b) Bastos, M. M.; Costa, C. C. P.; Bezerra, T. C.; de C da Silva, F.; Boechat, N. Efavirenz a nonnucleoside reverse transcriptase inhibitor of first-generation: Approaxhes based on its medicinal chemistry. *Eur. J. Med. Chem.* **2016**, *108*, 455−465.

(4) Shishido, Y.; Wakabayashi, H.; Koike, H.; Ueno, N.; Nukui, S.; Yamagishi, T.; Murata, Y.; Naganeo, F.; Mizutani, M.; Shimada, K.; Fujiwara, Y.; Sakakibara, A.; Suga, O.; Kusano, R.; Ueda, S.; Kanai, Y.; Tsuchiya, M.; Satake, K. Discovery and stereoselective synthesis of the novel isochroman neurokinin-1 receptor antagonist 'CJ-17,493'. *Bioorg. Med. Chem.* **2008**, *16*, 7193−7205.

(5) (a) Ma, J.-A.; Cahard, D. Update 1 of: Asymmetric Fluorination, Trifluoromethylation, and Perfluoroalkylation Reactions. *Chem. Rev.* **2008**, *108*, PR1−PR43. (b) Huang, Y.-Y.; Yang, X.; Chen, Z.; Verpoort, F.; Shibata, N. Catalytic Asymmetric Synthesis of Enantioenriched Heterocycles Bearing a C−CF_3 Stereogenic Center. *Chem. - Eur. J.* **2015**, *21*, 8664−8684. (c) He, X.-H.; Ji, Y.-L.; Peng, C.; Han, B. Organocatalytic Asymmetric Synthesis of Cyclic Compounds Bearing a Trifluoromethylated Stereogenic Center: Recent Developments. *Adv. Synth. Catal.* **2019**, *361*, 1923−1957.

(6) Ameen, D.; Snape, T. J. Chiral 1,1-diaryl compounds as important pharmacophores. *Med. Chem. Commun.* **2013**, *4*, 893−907.

(7) Wang, J.; Li, L.; Chai, M.; Ding, S.; Li, J.; Shang, Y.; Zhao, H.; Li, D.; Zhu, Q. Enantioselective Construction of 1H-Isoindoles Containing Tri- and Difluoromethylated Quaternary Stereogenic Centers via Palladium-Catalyzed C−H Bond Imidoylation. *ACS Catal.* **2021**, *11*, 12367−12374.

(8) (a) Lee, T.; Wilson, T. W.; Berg, R.; Ryberg, P.; Hartwig, J. F. Rhodium-Catalyzed Enantioselective Silylation of Arene C−H Bonds: Desymmetrization of Diarylmethanols. *J. Am. Chem. Soc.* **2015**, *137*, 6742−6745. (b) Su, B.; Zhou, T.-G.; Li, X.-W.; Shao, X.-R.; Xu, P.-L.; Wu, W.-L.; Hartwig, J. F.; Shi, Z.-J. A Chiral Nitrogen Ligand for Enantioselective, Iridium-Catalyzed Silylation of Aromatic C−H bonds. *Angew. Chem., Int. Ed.* **2017**, *56*, 1092−1096. (c) Su, B.; Hartwig, J. F. Development of Chiral Ligands for the Transition-Metal-Catalyzed Enantioselective Silylation and Borylation of C−H Bonds. *Angew. Chem., Int. Ed.* **2022**, *61*, No. e202113343.

(9) Zhang, H.; Zhao, D. Synthesis of Silicon-Stereogenic Silanols Involving Iridium-Catalyzed Enantioselective C−H Silylation Leading to a New Ligand Scaffold. *ACS Catal.* **2021**, *11*, 10748−10753.

(10) Yang, G.; Zhang, W. Renaissance of pyridine-oxazolines as chiral ligands for asymmetric catalysis. *Chem. Soc. Rev.* **2018**, *47*, 1783−1810.

(11) Ru-catalyzed intramolecular benzylic C−H silylation has been reported: Zuo, Z.; Xu, S.; Zhang, L.; Gan, L.; Fang, H.; Liu, G.; Huang, Z. Cobalt-Catalyzed Asymmetric Hydrogenation of Vinylsilanes with a Phosphine−Pyridine−Oxazoline Ligand: Synthesis of Optically Active Organosilanes and Silacycles. *Organometallics* **2019**, *38*, 3906−3911.

(12) The generation of hydridoiridium(I) species from chloroiridium(I) complexes and hydrosilanes has been proposed, see: (a) Song, L.-J.; Ding, S.; Wang, Y.; Zhang, X.; Wu, Y.-D.; Sun, J. Ir-Catalyzed Regio- and Stereoselective Hydrosilylation of Internal Thioalkynes: A Combined Experimental and Computational Study. *J. Org. Chem.* **2016**, *81*, 6157−6164. (b) Srinivas, V.; Nakajima, Y.; Sato, K.; Shimada, S. Iridium-Catalyzed Hydrosilylation of Sulfur-Containing Olefins. *Org. Lett.* **2018**, *20*, 12−15. (c) Zhang, X.; Gao, C.; Xie, X.; Liu, Y.; Ding, S. Thioether-Facilitated Iridium-Catalyzed Hydrosilylation of Steric 1,1-Disubstituted Olefins. *Eur. J. Org. Chem.* **2020**, *2020*, 556−560.

(13) (a) Harrod, J. F.; Gilson, D. F. R.; Charles, R. Oxidative addition of silicon hydrides to hydridocarbonyltris-(triphenylphosphine)iridium(I). *Can. J. Chem.* **1969**, *47*, 2205−2208. (b) Chalk, A. J. A New Synthesis of Silyliridium Hydrides. *J. Chem. Soc. D* **1969**, 1207−1208.

(14) Two pairs of hydride signals were observed when the stoichiometric reaction of $[IrCl(cod)]_2$ (1 equiv), **L6** (2 equiv), and **2b** (2 equiv) in THF-d_8 at 80 °C was monitored by ^{1}H NMR spectroscopy (see, Supporting Information).

(15) Trace amounts of H_2 was detected when the catalytic reaction of **2b** in THF-d_8 under the standard conditions was monitored by ^{1}H NMR spectroscopy (see, Supporting Information).

(16) Johnson, E. R.; Keinan, S.; Mori-Sánchez, P.; Contreras-García, J.; Cohen, A. J.; Yang, W. Revealing Noncovalent Interactions. *J. Am. Chem. Soc.* **2010**, *132*, 6498−6506.

(17) A similar Ir(III)/Ir(V) catalytic cycle was also proposed for a related dehydrogenative silylation: Zhang, M.; Liang, J.; Huang, G. Mechanism and Origins of Enantioselectivity of Ir-Catalyzed Intramolecular Silylation of Unactivated C(sp^3)−H Bonds. *J. Org. Chem.* **2019**, *84*, 2372−2376.

(18) Meanwell, N. A. Fluorine and Fluorinated Motifs in the Design and Application of Bioisosters for Drug Design. *J. Med. Chem.* **2018**, *61*, 5822−5880.

(19) A related tandem reaction, leading to (*Z*)-1-benzylidene-1,3-dihydroisobenzofurans, was reported: Zanardi, A.; Mata, J. A.; Peris, E. Domino Approach to Benzofurans by the Sequential Sonogashira/Hydroalkoxylation Couplings Catalyzed by New N-Heterocyclic-Carbene-Palladium Complexes. *Organometallics* **2009**, *28*, 4335−4339.

(20) Deposition number 2310281 (for **13**) contains the supporting crystallographic data for this paper.

https://doi.org/10.1021/jacsau.3c00794
JACS Au 2024, 4, 807−815